MIRSURG

Mid-Infrared Solid-State Laser Systems for Minimally Invasive Surgery

Grant agreement no.: 224042

Specific Targeted Research
Theme 3: **Information and Communication Technologies (ICT)**

D3.4: Mid-IR ns OPOs pumped at 1 µm

Due date of deliverable: month 42
Actual submission date: month 44

Start date of project:	01/06/2008
Duration:	3.5 years
Organisation name of lead contractor for this deliverable:	MBI Forschungsverbund Berlin e.V.: Max-Born-Institute

Project co-funded by the European Commission within the Seventh Framework Programme (2008-2011)		
Dissemination Level		
PU	Public	
PP	Restricted to other programme participants (including the Commission Services)	
RE	Restricted to a group specified by the consortium (including the Commission Services)	
CO	Confidential, only for members of the consortium (including the Commission Services)	CO

Index

1. Outline

The purpose of this deliverable is to describe the activities towards generation of high energy nanosecond pulses in the 6.45 μm spectral range by single step parametric frequency conversion starting from 1 μm Q-switched pump lasers. While from the very beginning it was clear that this approach cannot compete with single step conversion from the 2-μm spectral range (because of the ultimate quantum efficiency limit), for minimally invasive surgery on specific tissues (e.g. ophtalmologic surgery) it is expected that lower energy levels at 6.45 μm could be sufficient and such applications can profit from the extreme simplicity of this approach even at lower output powers. Its main advantage is that it is based on commercially available pump sources, basically Q-switched Nd-lasers and amplifiers. However, the great challenge was to acquire rather exotic nonlinear optical crystals which were provided from external collaborators because only very few such non-oxide materials exhibit sufficiently large band-gap to avoid two-photon absorption (TPA) at the pump wavelength of 1064 nm and simultaneously possess good transparency at 6.45 μm. In addituion, such materials exhibit relatively high residual losses and the necessary AR-coatings are still to a great extent in the development stage.

In the related Deliverable D1.8, we compared the properties of all potential candidates for direct single step frequency conversion and described our own results related to their characterization. Here we summarize all the efforts devoted to frequency conversion by optical parametric oscillators pumped at 1064 nm with nanosecond pulses. In all cases the same pump source has been employed: a commercially available diode-pumped Q-switched Nd:YAG laser (Innolas GmbH, Germany) delivering 10 mJ, 14 ns pulses at 100 Hz (10 W) which was upgraded in the third final period with an amplifier delivering 250 mJ, 8-ns pulses at 100 Hz (25 W). Its spectral linewidth amounted to 1 cm^{-1} and $M^2 \sim 1.4$.

The nonlinear crystals studied and the corresponding results can be grouped in 3 categories:

- $LiInSe_2$ (LISe): With this material previous experience existed, however it was limited to shorter idler wavelengths where oxide materials can also operate. In the experiments within MIRSURG the performance at longer wavelengths was studied, covering the 6.45 μm spectral range.

- $CdSiP_2$ (CSP): This material was discovered just when MIRSURG started. Many of its properties make it almost predestined for 6.45 μm generation although the tunability is limited. The extremely high nonlinearity of CSP made it possible to use it also without an OPO cavity, as an optical parametric generator (OPG). CSP is unique in the sense that it can be used under 90° non-critical phase-matching for the conversion process, however, unfortunately this configuration turned out incompatible with the RISTRA type cavity which was successfully employed by other partners (see Deliverables D3.6 and D3.7).

- Being very close to the band-gap of CSP with just 2 pump photons, we decided to test also nonlinear materials with extreme band-gap values (colourless) which exhibited much higher surface damage threshold (see Deliverable D1.8). Although OPO operation was obtained for the first time also with $LiGaS_2$ (LGS), much better results were achieved with $BaGa_4S_7$ (BGS) because this material could be provided in larger size. Note that BGS was discovered during the project and fully characterized within WP1.

2. LISE based OPOs

Nanosecond OPO operation with LISe crystals in the mid-IR wavelength range above 4 μm extending up to 8.7 μm for the idler wave, was achieved for the first time. Pumping at a repetition rate of 100 Hz and the absence of thermal effects allowed us to increase the average power by more than an order of magnitude at wavelengths much longer than in the initial demonstration. Further scaling is possible provided better polishing and AR-coating processes are developed. One of the main challenges, the reduction of the residual losses in the clear transparency range of LISe, however, remains because only after solving this problem the better thermo-mechanical characteristics of this material could be utilized in order to substantially outperform the more conventional chalcopyrite AGS.

Until the start of the MIRSURG project, nanosecond OPOs based on chalcogenides pumped in the 1 μm range, had been demonstrated only with Ag_3AsS_3, $AgGaS_2$ (AGS), $HgGa_2S_4$ (HGS), $LiInSe_2$ (LISe), and the solid solution $Cd_xHg_{1-x}Ga_2S_4$. Moreover, apart from the archive Ag_3AsS_3, oscillation at idler wavelengths exceeding 4.4 μm had been demonstrated only with AGS, achieving impressive tunability from 3.9 to 11.3 μm. First, we focused on the extension of the tuning range of a nanosecond LISe OPO to the mid-IR in order to cover the 6.45 μm spectral range, because experience with this material already existed at shorter wavelengths [1]. Moreover, an important task was to scale up the average power by increasing the repetition rate to 100 Hz. LISe is a non-oxide nonlinear crystal with better thermo-mechanical properties in comparison to the commercially available AGS whose band-gap (2.86 eV) and transparency allowed in the past nanosecond OPO operation in the mid-IR without TPA for a pump wavelength of 1064 nm. However, the first LISe based OPO had a limited tunability of 3.3-3.78 μm for the idler and the average idler power did not exceed 2.5 mW [1].

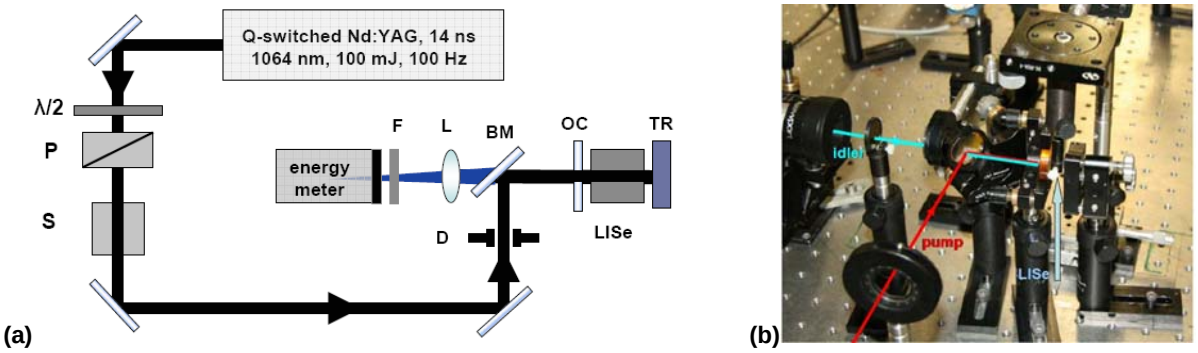

Figure 1: Experimental set-up of the LISe OPO (a). $\lambda/2$: half-wave plate, P: polarizer, S: mechanical shutter, F: 2.5 μm cut-on filter, L: 10 cm MgF_2 lens, D: diaphragm, BM: bending mirror, OC: output coupler, TR: total reflector. Photograph of the compact OPO set-up (b).

The OPO cavity used is shown in Fig. 1. It consisted of two plane mirrors with a separation between 18.5 and 27.5 mm, depending on the LISe crystal used. The rear total reflector, TR, was an Ag-mirror with a reflection of >98.5% at the pump, signal and idler wavelengths. In the tuning ranges studied, the output coupler, OC, had a transmission of 18-22% at the signal and ~73-84% at the idler wavelength, hence, the OPO can be considered as singly resonant with double pass pumping. However, the signal was not totally reflected by the output coupler to avoid extreme intracavity fluence that could damage the crystals. The LISe crystals were pumped through the output mirror which had a transmission of 82% at 1064 nm. The beams were separated by the pump bending mirror, BM, which had high reflection for the pump (R=98% for p-polarization) and transmitted ~67% (p-polarization) at the idler wavelength. Both the plane-parallel output coupler, OC, and the bending mirror, BM, were on ZnSe substrates with uncoated rear surfaces.

The pump laser generated 100 mJ, 14 ns (FWHM) pulses with an average power of 10 W. The energy stability was +/-1%. A mechanical shutter (S) with an aperture of 8 mm, operating up to 50 Hz (nmLaser, USA), was employed to reduce the repetition rate and thus the average pump power. A combination of a half-wave plate, $\lambda/2$, and a polarizer, P, served to adjust the pump energy. The pump laser was protected by a Faraday isolator and the separation to the OPO was large enough to avoid feedback during the Q-switching process. The pump beam was not focused and had a Gaussian waist (radius) of 1.9 mm in the position of the OPO. The output of the OPO, behind the bending mirror, BM, was detected by a calibrated

pyroelectric energy meter positioned in front of the focus of a 10-cm MgF_2 lens, L. Only the idler energy was measured, the residual pump radiation and the signal were blocked by a 2.5 μm cut-on filter, F.

The samples used in the present study, see Fig. 2a, were grown from oriented seeds by the vertical two-zone furnace Bridgman technique. They were cut for propagation in the *x*-*y* plane, type-II e-oe phase-matching, which is characterized by maximum effective nonlinearity d_{eff}. One sample (A) was cut at φ=41.6° for idler wavelength ~6.5 μm at normal incidence. It had an aperture of 5 mm (along *z*-axis) × 6.5 mm and a length of 17.6 mm. This sample was AR-coated with a single layer of YF_3 for high transmission at 1064 nm and in the 1.15-1.35 μm signal range (see Fig. 2b). We measured average surface reflectivity of 2.8% at 1064 nm and 1.8% at 1600 nm. From the measured transmission of 71% at 1064 nm and 85% at 1600 nm, we estimated effective absorption (including scatter) of 16%/cm at 1064 nm and 7%/cm at 1600 nm. The second sample (B) was cut at φ=34° for idler wavelength ~8.8 μm at normal incidence. It had an aperture of 5 mm (along *z*-axis) × 7 mm and a length of 24.5 mm. This sample was AR-coated with the same single layer for high transmission at 1064 nm and in the 1.15-1.35 μm signal range. However, due to some failure in the coating process, the difference in the residual reflectivity of the two surfaces was more pronounced. One surface had substantially higher (5% at 1064 nm and 4.5% at 1600 nm) reflection than the other (1% at 1064 nm and <1% at 1600 nm). From the measured transmission of 67.7% at 1064 nm and 82% at 1600 nm, we estimated for sample B, effective absorption (including scatter) of 14%/cm at 1064 nm and 6%/cm at 1600 nm, which is very similar to the estimates for sample A.

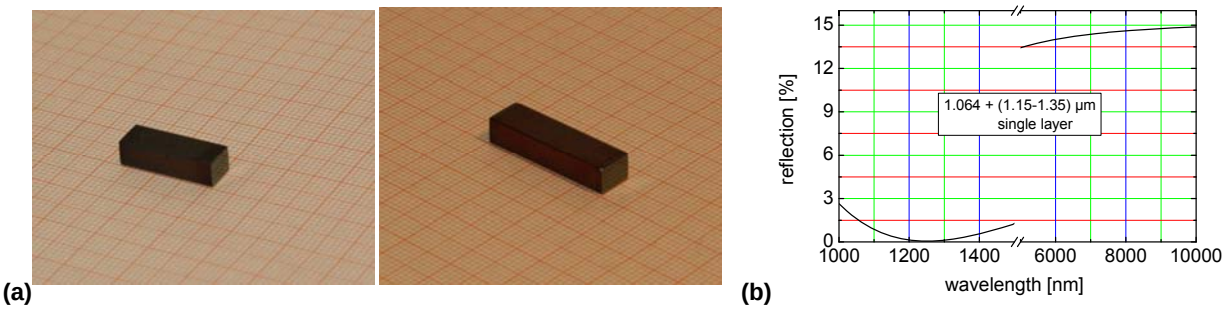

Figure 2: AR coated samples of LISe used (a): sample A (left) and sample B (right), see text. Single-layer AR-coating design (b).

We studied the input/output characteristics of the OPO, including the oscillation threshold, at normal incidence and minimum possible cavity length. The tuning curves required tilting of the crystals and the corresponding cavity length was slightly increased.

The thresholds measured for cavity length of 18.5 mm (sample A) and 25.5 mm (sample B) amounted to 6.8 mJ and 7.9 mJ, energy incident on the crystals, respectively. These values correspond to average fluence of 0.06 J/cm^2 and 0.07 J/cm^2 or pump intensity of 4.3 MW/cm^2 and 5 MW/cm^2. The peak on-axis values for the fluence and the intensity are two times higher. The threshold can be calculated by using Brosnan & Byer's formula for a singly resonant OPO with recycled pump [2]. We used the exact experimental parameters, correcting for the pump beam absorption after the first pass and assuming equal (averaged for signal and idler) absorption of 0.05 cm^{-1} for the resonated wave. From the nonlinear coefficients of LISe, rescaled using Miller's rule [3], we calculated an effective nonlinearity of d_{eff}=10.6 pm/V (φ=41.6°, sample A) and 11 pm/V (φ=34°, sample B). The results for the threshold pump fluence were 0.23 J/cm^2 and 0.15 J/cm^2 for sample A and B, respectively. These values correlate better with the experimental peak (on-axis) values which can be explained by the fact that oscillation starts in the central part of the pump beam. Deviations and the fact that sample B had in fact a higher oscillation threshold than sample A may have several reasons: the losses at the exact signal and idler wavelengths were unknown and we interpolated them to 6%/cm at the signal and assumed 4%/cm at the idler wavelength, eventually these losses, in particular for sample B, could be higher; besides for the pump, the residual reflections at the crystal faces were neglected; and finally the partial resonance of the idler is not taken into account by the theory. Having in mind all such assumptions, the correspondence between theory and experiment can be considered as satisfactory.

At a pump level of about two times the threshold we investigated the dependence of the output power on the repetition rate in the range 10-100 Hz. Fluctuations were within the experimental error and we conclude that there is no such dependence. This result was rather unexpected since the present samples

had in fact larger residual absorption than the one used in earlier work at shorter idler wavelengths [1]. This fact can be explained by the weaker thermal lensing in the case of larger beam sizes. The further measurements were performed at 100 Hz with the shutter removed (Fig. 3a).

The input/output characteristics for the two samples are shown in Fig. 3a. Maximum energies of 282 µJ at 6.514 µm and 116 µJ at 8.428 µm were measured. These values correspond to external quantum conversion efficiencies of 10.3% and 4.3%, respectively. The above wavelengths deviate from the calculated ones being longer for sample A and shorter for sample B. However, the deviations at the signal wavelengths, from the measurement of which the idler wavelengths were calculated, were only about 3 nm and 5 nm, respectively. The maximum average power at 100 Hz amounts to 28 mW. This is an improvement of more than an order of magnitude in comparison to earlier work, where ~2.5 mW at 3457 nm were achieved at lower repetition rates [1]. Since OPO operation with any chalcogenide crystal is confined to a narrow pump power range between the oscillation threshold and the damage threshold this fact emphasizes the importance of the good spatial profile and the pulse-to-pulse stability of the diode-pumped pump source.

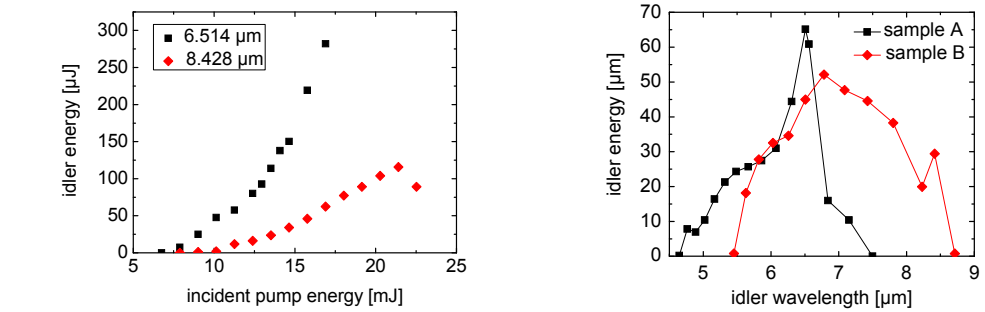

Figure 3: Output idler energy with LISe sample A (black squares) and sample B (red diamonds) versus pump energy at 1064 nm, incident on the crystals (a). Curves recorded at normal incidence with cavity length of 18.5 and 25.5 mm, respectively. The last point in case B denotes surface damage. Tuning OPO curves recorded for the two LISe samples at fixed pump energy (b).

The OPO linewidth was measured at the signal wavelength of 1272 nm using a 1-mm-thick Ag-coated CaF_2 Fabry-Perot etalon. It was ~58 GHz (~1.9 cm^{-1}). This is 2 times less than the spectral acceptance for the three-wave nonlinear process assuming narrow-band pump. The pulse-to-pulse stability for the idler pulses measured at maximum output level was +/-5%. The pulse duration at the same signal wavelength measured with a fast (0.7 ns) InGaAs photodiode was 7 ns.

The tuning curves (Fig. 3b) were recorded by lengthening the cavity to 20.5 mm (sample A) and 27.5 mm (sample B) and tilting the crystals in the critical plane (rotation about the *z*-axis). The pump energy was 11.8 mJ for sample A and 16.9 mJ for sample B. The upper limit of the tunability is determined by the LISe absorption which, for such sample lengths, sets on from about 8 µm, and is not related to the optics used (the thin MgF_2 lens was substituted by a BaF_2 lens to check this). The point which deviates from the smooth dependence for sample B is near 8.428 µm, corresponding to normal incidence, which can be explained by some enhancement of the feedback by the partial reflection of the crystal faces. Thus we showed that the full transparency range of LISe can be utilized using an OPO pumped at 1064 nm.

Surface damage was observed with both OPO active elements. It can be only speculated why damage of the two OPO samples in the form of whiter surface spot occurred at much lower pump energy (10-15 mJ) inside the cavity. Complete damage was also observed at lower levels (15-20 mJ) but could be a consequence of already existing whiter spot. There are two possibilities: either contribution from the resonated signal wave (as reported for other crystals) or simply low quality of this AR-coating. Experiments outside the cavity indicated lower damage of the surface with higher residual reflection, also lower threshold for whitening, so it seems more probable that this surface was simply of lower quality and that is why it got damaged although it was not always the front surface in the OPO.

3. Parametric down-conversion using CSP

3.1 Linear CSP OPO

CSP was employed in a nanosecond, 90°-phase-matched singly resonant OPO pumped at 1064 nm, to produce idler pulses near 6.2 μm with an energy as high as 470 μJ at 10 Hz and average power as high as 9.1 mW at 20 Hz. The power limit was set by AR-coating damage.

Our work within WP1 showed that the newly discovered CSP crystal is extremely interesting for realization of unique non-critical OPO pumped at 1064 nm for direct generation of idler radiation near 6.45 μm. The sample used in the initial study (sample 17A, Fig. 4) was cut at θ=90°, φ=45° and had a length of 8 mm. Its aperture was 6 mm (along the *c*-axis) × 6.75 mm. The residual losses measured for the relevant polarizations (e for the pump and o for the signal and idler) are 0.198 cm^{-1} at 1064 nm, 0.114 cm^{-1} near 1.3 μm, and 0.014 cm^{-1} near 6.2 μm. Both faces were AR-coated for the three wavelengths (pump, signal, and idler) and the 8-layer coating (TwinStar, USA) resulted in averaged reflectivities per surface of ~0.35% at 1.064 μm, ~0.4% at 1.285 μm and ~0.5% at 6.2 μm.

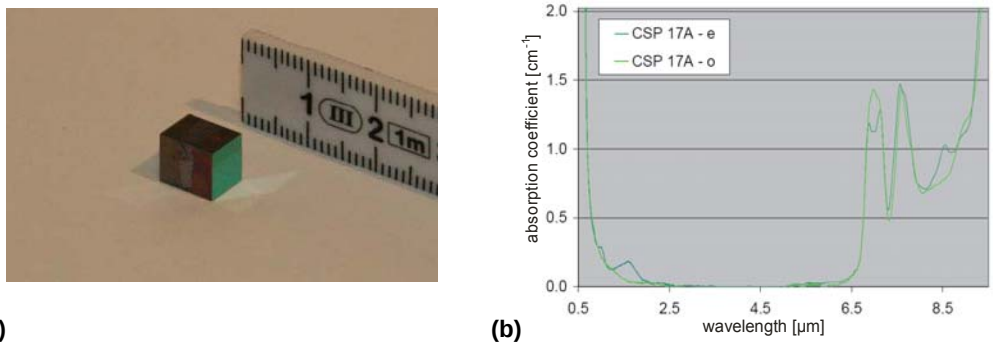

(a) **(b)**

Figure 4: The AR-coated CSP 17A sample used (a) and its polarized transmission measured prior to coating (b).

The OPO cavity used was similar to the one described previously about LISe, see Fig. 1. It consisted of two plane mirrors with a separation of 9.5 mm. The rear total reflector, TR, was an Ag-mirror with a reflection of >98.5% at the pump, signal and idler wavelengths. The output coupler, OC, had a transmission of 20% at the signal and 75% at the idler wavelength, hence, the OPO can be considered again as singly resonant with double pass pumping. Similarly, the signal was not totally reflected by the output coupler to avoid extreme intracavity fluence that could damage the crystal. The CSP crystal was pumped through the output mirror which had a transmission of 82% at 1064 nm. The beams were separated by the pump bending mirror, BM, which had high reflection for the pump (*R*=98% for p-polarization) and transmitted 37% and 64% (s-polarization) at the signal and idler wavelengths, respectively. Both the plane-parallel output coupler, OC, and the bending mirror, BM, were on ZnSe substrates with uncoated rear surfaces. The same pump source was used and again the pump beam was not focused and had a Gaussian waist of ~1.9 mm in the position of the OPO.

Only normal incidence was studied in this configuration since the cavity was as short as possible in order to reduce the OPO threshold. In this non-critical scheme, the measured signal wavelength was 1.285 μm, corresponding to an idler wavelength of 6.193 μm. The calculation using the refined Sellmeier equations gives an idler wavelength of 6.18 μm but this slight deviation corresponds to only 0.6 nm at the signal wavelength which is below the accuracy of the spectrometer. This is a good confirmation for the reliability of the existing Sellmeier equations. The duration of the signal pulse, measured by a fast InGaAs photodiode, was 10 ns.

The pump threshold was about 1.8 mJ (~16 mJ/cm^2). The threshold was calculated again by using Brosnan & Byer's formula for a singly resonant OPO with recycled pump [2]. We used the exact experimental parameters, correcting for the pump beam absorption after the first pass and assuming equal (averaged for signal and idler) absorption of 0.064 cm^{-1} for the resonated wave. The nonlinear coefficient d_{36} of CSP was rescaled using Miller's rule which gives an effective nonlinearity of d_{eff}=92.3 pm/V for this process [3]. The result for the threshold pump fluence was 29 mJ/cm^2. This value correlates better with the experimental peak (on-axial) fluence (~32 mJ/cm^2) which can be explained by the fact that oscillation starts in the central part of the pump beam. Then the estimated threshold in terms of energy would be 1.65 mJ. Note that the fact that the idler is also resonated to some extent (100%

reflected by the rear mirror and 25% reflected by the output coupler) is not taken into account in that model.

The maximum idler energy measured at 10 Hz repetition rate was 0.47 mJ, at an incident pump energy of 21.4 mJ. This gives a conversion efficiency of 2.2% for the idler alone or a quantum conversion efficiency of ~12.8%. Only slightly lower output energies were observed at 20 Hz which can be attributed to the residual crystal absorption at the pump wavelength. The maximum average output power (idler only), reached in this case, was 9.1 mW. The measurements in Fig. 5a extend to an upper limit, where surface damage to the AR-coating of the input face was observed. In terms of average fluence (~0.22 J/cm^2), the damage threshold is similar to that reported for AGS. Since the expectations for CSP are much higher, we believe the present damage is related to the AR coating. Single-layer coating is believed to solve this problem. Nevertheless, the output energy level achieved with this very first sample of CSP already exceeded the best result previously reported at such long wavelengths with ~1 µm pumped OPOs, namely 372 µJ at 6 µm using AGS [4]. Moreover, the input/output characteristics in Fig. 5a show no saturation, in contrast to the AGS performance, which means that power scaling can be expected even without increasing the pump beam diameter.

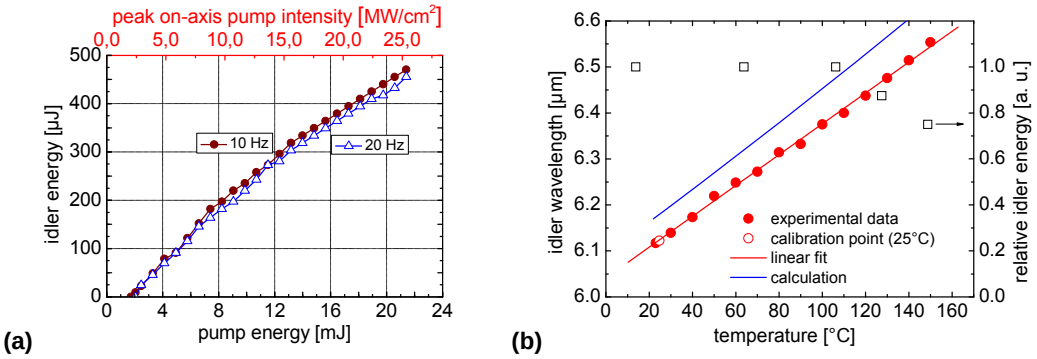

Figure 5: Idler output energy vs. incident pump energy on the OPO crystal for two repetition rates (a) and temperature tuning in the non-critical configuration of CSP (b).

The OPO linewidth, measured at the signal wavelength using a 1-mm-thick Ag-coated CaF_2 Fabry-Perot etalon, was ~52 GHz (~1.7 cm^{-1}). This is roughly 3.5 times less than the spectral acceptance for the three-wave nonlinear process. The pulse-to-pulse stability for the idler pulses measured at an output level of 350 µJ was +-5%.

Using an analogous sample of CSP, 9.5 mm in length (sample 17B), and a very similar cavity we were able to extend the above results to sub-nanosecond idler pulse durations using a special 1 ns pump source at 1064 nm. This was possible due to the short OPO cavity length. We will not go here into details because this OPO operated at 1 kHz but will only mention that at similar conversion efficiencies, a maximum output power of 24 mW (24 µJ) was achieved without any damage to the sample up to a peak on-axis intensity of 32 MW/cm^2. This set-up was designed, however, with a special temperature controller and we were able to study the temperature tuning from room temperature to 150°C, see Fig. 5b. To accommodate the oven, the cavity length had to be increased to 11 mm. All four lateral surfaces of the crystal were in good thermal contact with the metal holder which was heated and where the temperature was measured by a calibrated sensor. The idler wavelengths were calculated from the signal wavelengths measured with a low resolution (~10 nm) InGaAs spectrometer (Avantes Model NIR256-1.7). Tuning from 6.117 to 6.554 µm was obtained for the idler wavelength. Thus CSP possesses nice tuning capability under non-critical conditions which allows one to utilize its transparency up to the intrinsic limit set by multiphonon absorption. Note that in the well known, but optically positive nonlinear crystal $ZnGeP_2$ (ZGP) which, as CSP, belongs to the II-IV-V_2 chalcopyrite class, the temperature tuning is very limited, e.g. 1 nm/deg for type-II non-critical configuration and 2.79 µm pump, which is obviously of no practical importance. From Fig. 5b it is clear that CSP is far more tunable than ZGP and recent OPO experiments at BAE Systems with critical phase-matching and 1.99 µm pump wavelength (Tm-laser) show that the temperature tuning coefficient could be an order of magnitude (~10 nm/deg) higher than in ZGP.

The calibration point at 25°C in Fig. 5b corresponds to measurement of the frequency doubled (in a 5-mm type I BiB_3O_8 crystal) signal by a high resolution (0.25 nm) visible spectrometer. The calibration of this spectrometer (Acton Model SpectraPro 2150i) was confirmed by a He-Ne laser whose wavelength is very close to the second harmonic measured. The blue line in Fig. 5b shows a calculation based on

extrapolation of recently obtained temperature-dependent Sellmeier equations, derived from refractive index measurements in the 95-295 K range. The deviations in Fig. 5b amount to 60…100 nm for the idler wavelength and in terms of temperature they are of the order of 20 K. However, at the signal wavelength, the discrepancy between experiment and calculation is only 3…3.5 nm. Note that similar deviation of the wavelengths observed exists also with respect to the low-repetition-rate OPO described above. It is unclear if this is not a consequence of slight deviation in the sample stoichiometry.

The output idler energy is almost constant when changing the temperature, slightly decreasing above 6.4 µm, partially due to the idler absorption (Fig. 4b), to 75% of its maximum value, towards the longest idler wavelength achieved, see Fig. 5b.

The above results present first OPO demonstrations with CSP pumped at 1064 nm. Future progress will depend essentially on the availability of samples with reduced residual loss and improvement of the crystal surface damage resistivity. New cavity designs for maximum extraction of the idler energy, and power scaling using crystals of larger aperture are discussed in the following subsections.

3.2 RISTRA CSP OPO

The beam quality of the idler output of a 1064 nm pumped OPO based on CSP was compared for linear and Rotated Image Singly-Resonant Twisted RectAngle (RISTRA) cavities. For similar mirrors and cavity round trip times the RISTRA cavity yielded 64 µJ of idler energy (6.4 mW of average power at 100 Hz) compared to 34 µJ with the linear cavity, at a pump level of 21.5 mJ, roughly two times above threshold. The RISTRA cavity generated a somewhat smoother idler beam spatial profile (characterized by moving a knife-edge) and the intensity in the focus of a 10-cm lens was about 50% higher.

Regarding the eventual fiber coupling of the 6.45 µm radiation the demands on the OPO beam quality are not very high. Nevertheless, a good OPO efficiency is coupled to both, the beam quality of the pump and the one of the OPO signal and idler beams. This will be difficult in a standard two-mirror OPO cavity associated with a large Fresnel number $F = D^2/\lambda L$ due to the short OPO cavity length L and the large beam diameter D needed to avoid optical damage (λ denotes the resonated wave). The problem is quite critical especially for CSP since the combination of high effective nonlinearity and residual losses at the pump and signal wavelengths (these losses are not intrinsic to CSP but have still to be suppressed in an improved growth process) naturally leads to selection of shorter OPO active elements (of the order of 1 cm) while power/energy scaling would require large beam diameters to avoid not only surface damage but also saturation effects. Pumping with shorter pulses on the other hand also helps reaching the OPO threshold before optical damage occurs (since the latter is fluence dependent) and cavities should be as short as possible to ensure sufficient number of round trips.

Thus, a special OPO cavity geometry is needed for optimum performance. The design of such a cavity geometry has been shortly described as a non-planar four-mirror cavity with image-rotation [5]. The image rotation, working in conjunction with crystal birefringence, significantly improves the spatial quality of the beam even at large pump spot diameters [5,6]. The special OPO cavity design called RISTRA (Rotated Image Singly-Resonant Twisted RectAngle) makes an intracavity image rotation, the pumped region is thus better utilized by the oscillating signal and a much more uniform phase is obtained across the beam, leading to a more symmetric beam shape. The principle of image rotation works in conjunction with angle critical birefringent phase-matching to increase phase front correlation across the beam profile. With this technique the beam is spatially averaged. Image rotation is particularly effective for improving beam quality in high energy OPOs, where the ratio of beam diameter to cavity length results in a cavity Fresnel number that can be intentionally large. The detailed description of this principle, which has already been verified experimentally, can be found in the literature [5-7].

The RISTRA concept is not wavelength dependent and thus suitable for generation of idler wavelengths at 6.45 µm. It was originally implemented with single-frequency operation and type-II interaction, yielding optimum performance with flat-top pump (and seed) spatial profiles. However, type-I interaction and broadband unseeded operation with ZGP pumped at 2.05 µm with a Gaussian spatial distribution showed also very promising results in terms of conversion effciency and signal beam (at 3.4 µm) spatial quality [7]. Unfortunately no information on the idler output was presented in this paper.

We investigated the feasibility of the RISTRA concept for a 1064 nm pumped OPO based on CSP. We compared the idler beam quality for similar mirrors and cavity round trip times using a RISTRA cavity and a linear cavity. Type-I interaction is used for CSP and the RISTRA concept is tested for the fist time under 90°-phase-matcing.

The CSP sample 17B used in the present study (Fig. 6a) was very similar to 17A described before and cut at θ=90°, φ=45° with a length of 9.5 mm. Its aperture was 6 mm (along the *c*-axis) × 6.75 mm. The crystal *c*-axis and the pump polarization were in the horizontal plane (oo-e interaction). The residual losses measured for the relevant polarizations (e for the pump and o for the signal and idler) are 0.185 cm^{-1} at 1064 nm, 0.114 cm^{-1} at 1.3 µm, and 0.014 cm^{-1} at 6.2-6.4 µm. Both faces were AR-coated for the three wavelengths (pump, signal, and idler) and the 8-layer coating (TwinStar) had average reflectivity per surface of ~0.35% at 1064 nm, ~0.4% at 1275 nm, and ~0.8% at 6.4 µm. A measurement prior to the OPO experiment gave a transmission of 77% at 1064 nm for the AR-coated sample.

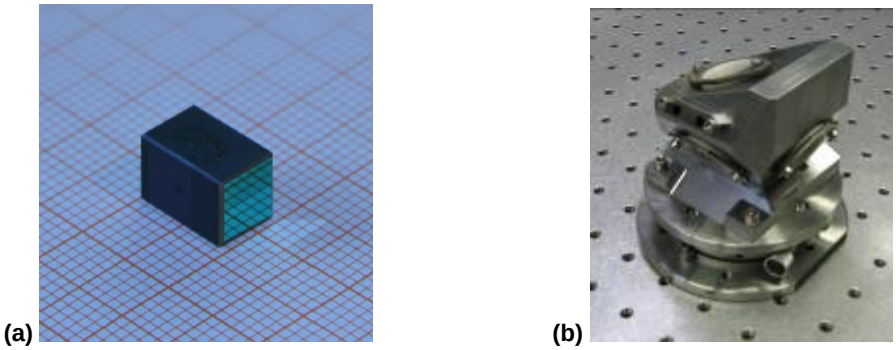

Figure 6: Photographs of the AR-coated CSP sample (a) and the RISTRA OPO cavity (b).

The RISTRA cavity, fabricated by the partner ISL, is shown in Fig. 6b. It contained an input coupler, HT at 1064 nm and 6125 nm for the pump and idler and HR at 1288 nm for the signal (in all cases for an angle of incidence of ~32.8°), and an output coupler, with similar specifications at the pump and idler wavelengths but with partial reflectivity for the signal wavelength (78% for s-polarization and 72% for p-polarization at the same angle of incidence of ~32.8°). The mirrors were on 1" diameter ZnSe substrates, 1/8" thick (TwinStar) and their rear surfaces were AR-coated for the pump and idler radiation. The remaining two RISTRA bending mirrors were of the same kind as the input coupler. Thus only the signal is resonated in the cavity and the pump beam passes just once through the CSP crystal. The physical RISTRA cavity length was 128 mm which corresponds to an optical length of *L*~147 mm.

The physical cavity length of the linear OPO cavity was 55 mm, so that a double pass through the CSP crystal corresponds to an optical length of *L*=148 mm, almost the same as for the RISTRA cavity. The linear cavity was also pumped in single pass and only the signal was resonated. As an input mirror we used the same input coupler as for the RISTRA cavity since we established that it is HR for the signal wavelength also at normal incidence and the transmission at the pump wavelength was still sufficiently high. As an output coupler for the linear cavity we used a 1" diameter dielectric mirror on a ZnS substrate (TwinStar) with 70% reflectivity for the signal wavelength, HT and with AR-coatings on the rear surface for the pump and idler wavelengths.

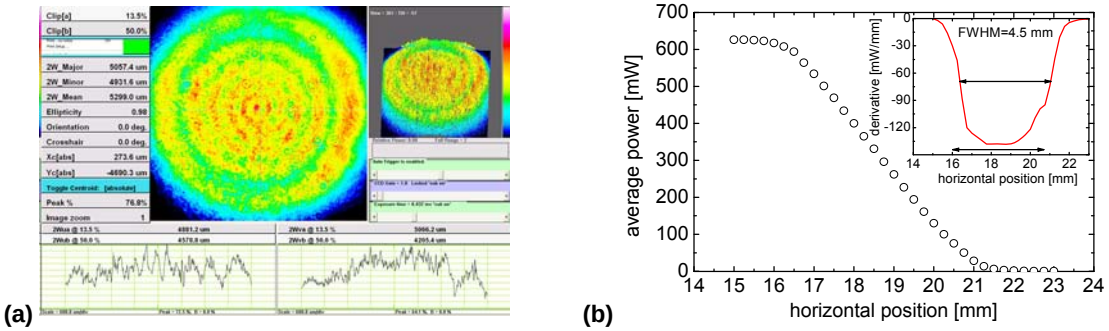

Figure 7: CCD image of pump spatial profile after the aperture (a) and measurement by the knife-edge method (b).

The same pump source was used delivering 100 mJ, 14 ns (FWHM) pulses at 1064 nm with an average power of 10 W. The pump beam exhibited quasi-Gaussian spatial profile with $1/e^2$ diameters of $2w_X$ = 5.5 mm and $2w_Y$ = 4.2 mm in the horizontal and vertical planes, respectively. After expanding the beam with a telescope consisting of two lenses (-40 mm and +75 mm), these diameters increased to $2w_X$ = 9.8 mm and $2w_Y$ = 8.1 mm, respectively. The pump beam was then passed through a circular aperture to obtain a

quasi-flat top spatial distribution. The spatial profile after the aperture was characterized by a CCD camera (Fig. 7a shows an image and two cross sections) and by the knife-edge method, calculating the first derivative of the measured average power dependence as a function of the horizontal coordinate (Fig. 7b). The latter measurement provides a rather smooth distribution but this is due to the integration of the power in the vertical direction. The spatial distribution is globally flat but locally modulated by diffraction rings. As can be seen from Fig. 7, the obtained pump beam size is optimum for filling the available CSP crystal aperture. The Fresnel number F $=D^2/\lambda L$ is ~100. Note that this number can be roughly 10 times higher in a short cavity OPO as the one used in the previously described OPO set-up using CSP.

Since the input couplers had different transmission at the pump wavelength, to compare the two cavities we studied the dependence on the pump energy incident on the CSP crystal. The maximum available pump energy incident on the CSP crystal was about 21.5 mJ in the case of the linear cavity, hence, we set the same upper limit also for the RISTRA cavity. The calculated pump intensity values correspond to the axial pump intensity, calculated from the measured incident energy by taking into account the aperture transmission (~1/2.7), the quasi-Gaussian beam spatial profile in front of the aperture, and the pump pulse duration of 14 ns.

Figure 8 shows the dependence of the idler output energy on the incident pump energy for the RISTRA and linear OPO cavities. The RISTRA pump threshold was 10.5 mJ corresponding to on-axis pump intensity of 6.4 MW/cm^2. The RISTRA cavity yielded a maximum idler pulse energy of 64 µJ (6.4 mW of average power at 100 Hz) compared to 34 µJ with the linear cavity, at a pump level of 21.5 mJ, in both cases roughly two times above the OPO threshold.

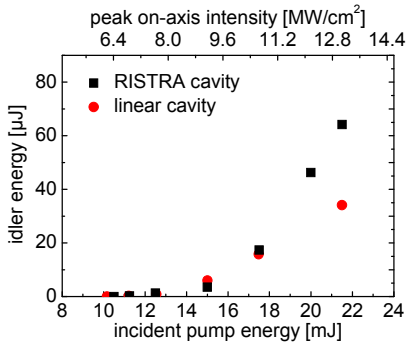

Figure 8: Idler pulse energy versus pump energy incident on the CSP crystal.

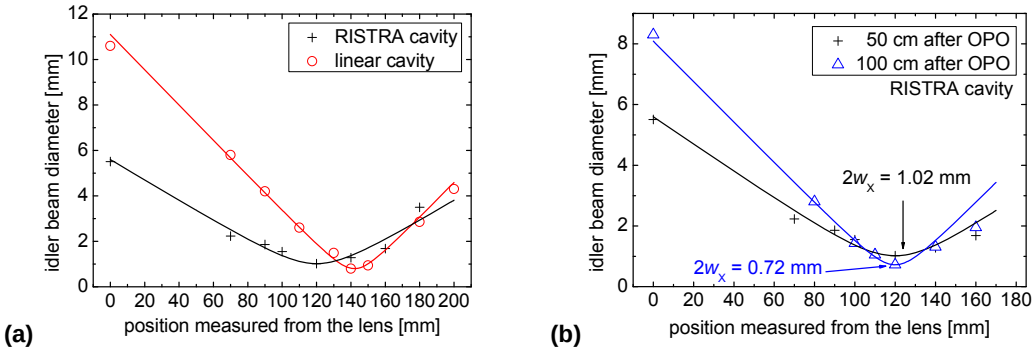

Figure 9: Idler beam horizontal diameter dependence on the position after a 10-cm focusing lens. Comparison between RISTRA and linear cavity with the lens at 50 cm from the OPO output coupler (a) and RISTRA cavity idler focusability with the 10-cm lens positioned at 50 and 100 cm from the OPO output coupler (b).

At first we evaluated the idler beam diameter by the knife-edge method using a 10-cm focal length BaF_2 lens positioned at 50 cm from the OPO output coupler (Fig. 9a). The beam waists obtained were similar for the linear and RISTRA cavities but the beam diameter on the lens was roughly two times smaller in the case of the RISTRA cavity due to the smaller divergence in this case. For a fair comparison we increased then the separation of the lens from the output coupler to 100 cm and the corresponding results are shown in Fig. 9b. The idler beam diameter at the position of the lens corresponds to abscissa zero. The idler beam diameter just after the RISTRA cavity was about 4 mm.

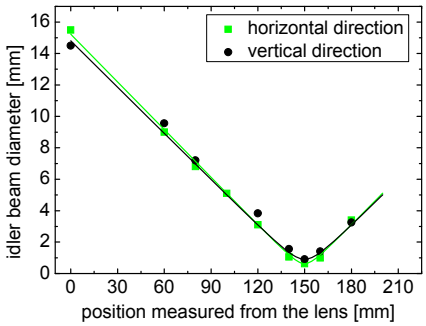

Figure 10: Idler beam diameter dependence measured with fully illuminated focusing lens with focal length of 10 cm.

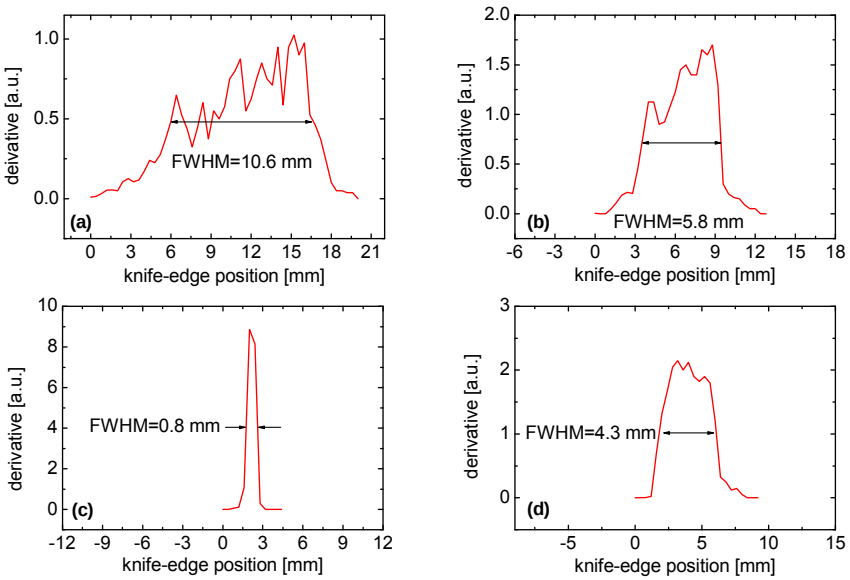

Figure 11: Idler beam profile and diameters in horizontal direction at several points after the 10-cm BaF_2 focusing lens, positioned 50 cm from the output coupler of the linear OPO cavity. (a) on the lens, (b) 7 cm after the lens, (c) 14 cm after the lens (focal point), and (d) 20 cm after the lens.

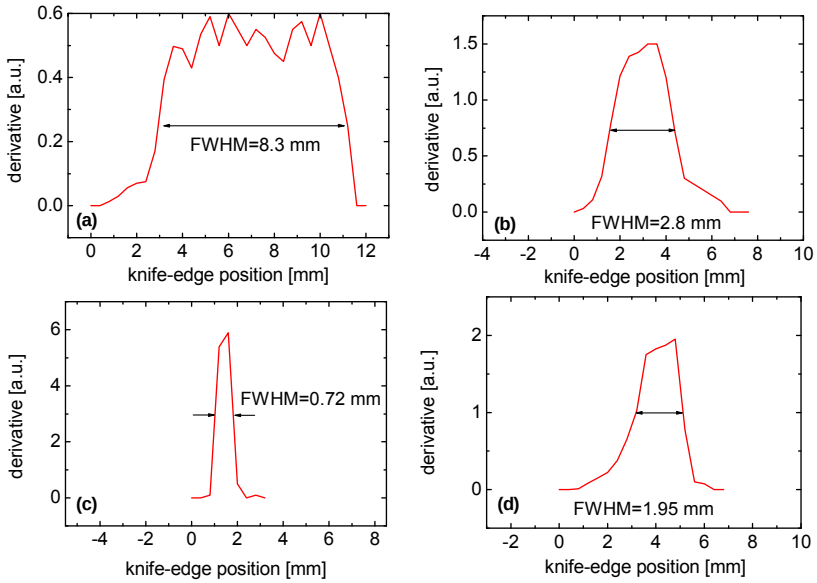

Figure 12: Idler beam profile and diameters in horizontal direction at several points after the 10-cm BaF_2 focusing lens, positioned 100 cm from the output coupler of the RISTRA OPO cavity. (a) on the lens, (b) 8 cm after the lens, (c) 12 cm after the lens (focal point), and (d) 16 cm after the lens.

To obtain minimum beam diameter in the focal spot, we expanded the idler beam after the RISTRA OPO to fill almost completely the aperture of the 10-cm BaF_2 focusing lens. The idler beam diameter on the lens amounted to ~15 mm (FWHM). The beam diameters in the horizontal and vertical planes were measured at several positions after the lens. The results are plotted in Fig. 10. The minimum obtained focal diameters were $2w_X$=630 μm and $2w_Y$=910 μm, in the horizontal and vertical directions, respectively.

In Figs. 11 and 12 we compare the idler beam profiles from both cavity configurations for the same beam diameter on the focusing lens. Figure 11 refers to the linear cavity with the 10-cm focusing lens at 50 cm from the output coupler and Fig. 12 refers to the RISTRA cavity with the 10-cm focusing lens at 100 cm from the output coupler It can be seen that the RISTRA cavity produces slightly more uniform idler beam spatial profile.

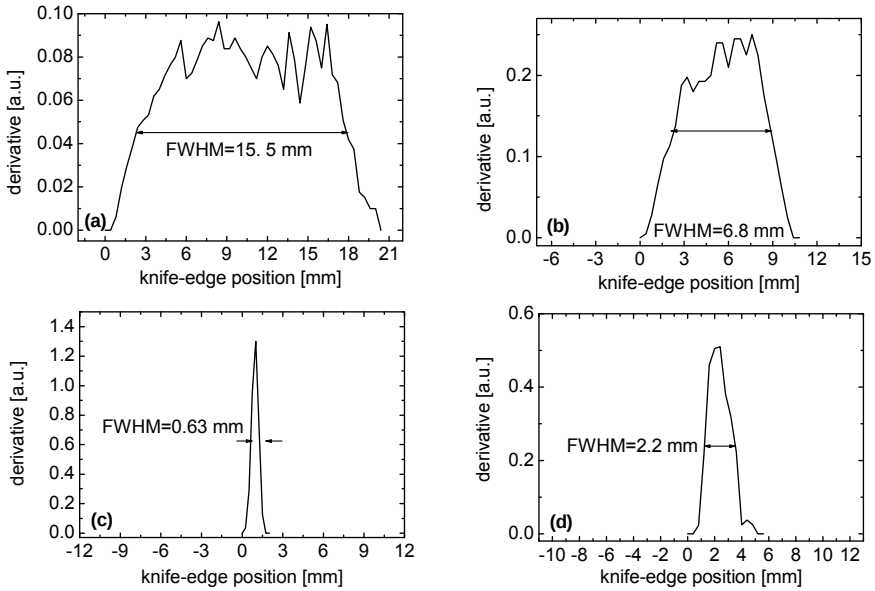

Figure 13: RISTRA OPO idler beam profile and diameter in the horizontal direction at several points after the fully illuminated 10-cm BaF_2 focusing lens. (a) on the lens, (b) 8 cm after the lens, (c) 15 cm after the lens (focal spot), and (d) 18 cm after the lens.

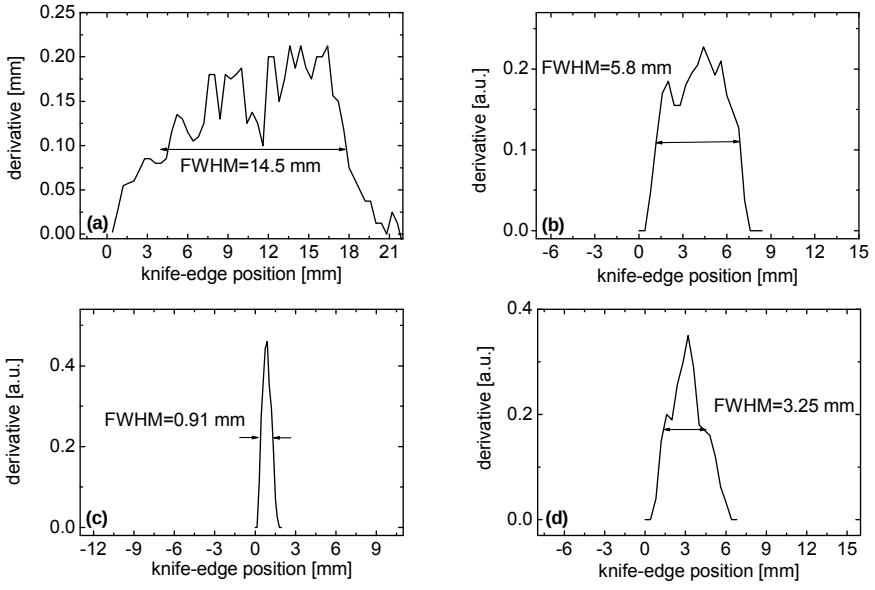

Figure 14: RISTRA OPO idler beam profile and diameter in the vertical direction at several points after the fully illuminated 10-cm BaF_2 focusing lens. (a) on the lens, (b) 8 cm after the lens, (c) 15 cm after the lens (focal spot), and (d) 18 cm after the lens.

Finally, in Figs. 13 and 14 we have plotted the idler beam profiles from the RISTRA cavity with the beam expanded to fully illuminate the 10-cm focusing lens. These plots correspond to the data in Fig. 10. Comparing the focal spot sizes achievable with the two cavities, only about 50% enhancement in the maximum achievable intensity is observed in the case of the RISTRA cavity.

The improvement in the spatial quality of the idler beam employing the RISTRA cavity was marginal in the low conversion limit studied (pump exceeding the threshold not more than twice) although the conversion efficiency was somewhat better. Since the RISTRA concept has previously been proven to be useful under similar conditions with type-I interaction, the absence of angle birefringence in non-critical 90° phase-matching is considered to be the main reason for the marginal spatial quality improvement observed in the present study.

3.3 CSP OPG

A 21.4-mm-long non-critically cut CSP crystal, pumped by 8-ns pulses at 1064 nm in a double-pass configuration for pump, signal and idler generated 523 μJ, 5.8-ns idler pulses at 6.125 μm. The average power of 52.3 mW at the repetition rate of 100 Hz is the highest ever achieved at such wavelengths with direct down-conversion from the 1-μm spectral range.

Efficient parametric frequency down-conversion at low (such as 100 Hz) repetition rates relies normally on nanosecond OPOs employing a resonant cavity but can be also achieved with optical parametric generators (OPGs) employing a single-pass traveling-wave scheme. Cavity is in general necessary for low peak pump powers, normally associated with pulses of duration from few nanoseconds to continuous-wave in which case many round trips of the resonated wave (signal or idler, or both) ensure sufficiently high parametric gain to reach threshold. Single-pass traveling-wave type OPGs on the other hand could only reach threshold with the high peak power available from ultrafast (femtosecond or picosecond, up to ~1 ns) amplified pump sources operating at lower repetition rates for which anyway an OPO cavity would be impractical (1 ns corresponds to 30 cm in free space). Ultrashort pulses would not be useful for the envisaged in the present project application because at the targeted energies higher order nonlinear effects will occur. However, it can be expected that in general, for pulse durations between 1 and 10 ns, high-gain nonlinear materials can be employed both in OPO and OPG configurations. The advantage of OPGs is that seeding is much easier to apply for narrow-band single-frequency operation.

We realized OPG operation at 100 Hz with the new nonlinear crystal CSP which possesses extremely high (84.5 pm/V) second-order nonlinear coefficient for non-critical birefringent phase-matching [3]. The CSP crystal available for this experiment (BAE Systems) was 21.4 mm long with an aperture of 4.1 (along *c*-axis) × 6.1 mm^2 and cut for non-critical (90°) type-I (oo-e) interaction, Fig. 15. Both faces were AR-coated with a single layer of sapphire (TwinStar) which in fact was optimized only for the pump and signal wavelengths (minimum reflection of ~1% at 1150 nm), hoping in this way to achieve higher surface damage threshold. The actual reflectivity measured at the three wavelengths was 1.3% (1064 nm), 2% (1288 nm), and 20% (6.125 μm).

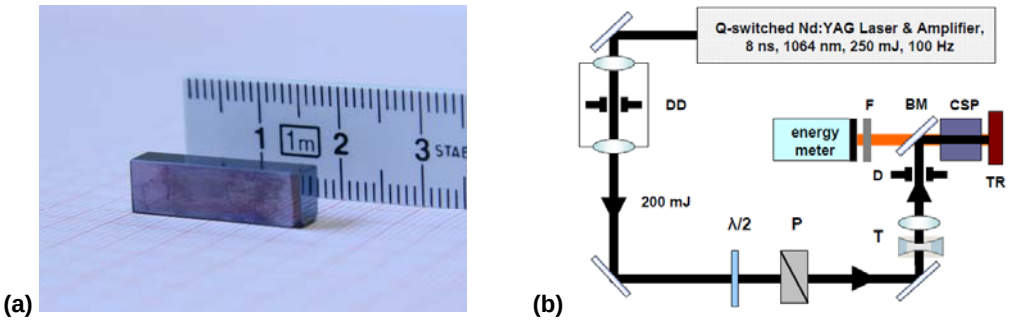

Figure 15: Photograph of the AR-coated CSP sample (a) and OPG set-up (b). T: telescope, D: diaphragm, BM: bending mirror, TR: total reflector, F: exchangeable filters, P: polarizer, λ/2: half-wave plate, DD: diamond diaphragm for spatial profile cleaning.

The pump beam from the upgraded diode-pumped Q-switched Nd:YAG laser / amplifier system operating at 100 Hz, after spatial filtering and attenuation by a system of wave plate and polarizer, was expanded to a slightly elliptical shape with approximately Gaussian spatial distribution and diameter of ~10.4 and

~12.1 mm in the horizontal and vertical (along the crystal *c*-axis) directions, respectively. A nearly flat-top spatial profile was then obtained by a circular aperture which reduced the beam diameter to ~3.8 mm, matching the limited crystal aperture. The pump pulse duration was 8 ns.

The CSP crystal was pumped in double-pass using a 45° ZnSe bending mirror for the pump radiation which was highly transmitting at both, signal and idler wavelengths, and a metal (Ag, R>98%) mirror to retro-reflect all the three pulses for a second pass, see Fig. 15. All separations were kept as short as possible to avoid air absorption of the idler.

The OPG threshold was found at 213 μJ of incident pump energy (~0.23 MW/cm^2 peak on-axis intensity), see Fig. 16a. At the maximum applied pump energy of 12 mJ (12.7 MW/cm^2), the total output energy exceeded 4 mJ, from which ~3.64 mJ were at 1288 nm (signal) and ~0.52 mJ at 6.125 μm (idler). The fluctuations were ±5%, measured for the idler. There was some trend of saturation of the idler energy – the ratio of the signal to idler energy increases with the pump level reaching ~7 at maximum level, while the theoretical value (without taking into account the different reflection of the crystal AR-coatings) should be around 4.8. There is still no explanation for this power dependent loss of idler energy.

The threshold obtained in terms of pump intensity is extremely low even having in mind the long pump pulse duration. The lowest known OPO pump threshold in terms of pump energy, is 2 μJ at 3.1 μm for pumping a non-critically cut 24-mm long type-II ZGP crystal which has similarly high nonlinearity [8]. This OPO utilized double pump pass and only the signal was resonated. In terms of pump fluence and intensity for the 10-ns long pulses at 3.1 μm the 2 μJ threshold energy is equivalent to 8.2 mJ/cm^2 and 0.82 MW/cm^2, respectively. Thus, in fact, the threshold measured in the present experiment with CSP is roughly four times lower, 1.84 mJ/cm^2. Note that an OPG should in general exhibit a higher threshold than an OPO.

Obviously, residual reflections may contribute to an OPO feedback effect. This was checked by tilting the crystal in order to facilitate non-collinear interaction and the conclusion was that the surface reflections formed a low-finesse cavity for the idler. This could be expected since the AR-coating was not optimized for the idler wavelength and the residual reflection was substantially higher than for the signal. Thus, the present experiment corresponds more or less to quasi-OPG or weakly-resonant OPO operation. Since optimization of AR-coatings for extremely low reflectivity at both signal and idler wavelengths requires multi-layers which is related to decreasing damage resistivity, better AR-coatings are not expected to suppress totally the OPO effect. On the other hand, wedged sample will not work either because the aperture of the CSP crystal is relatively large. A pure OPG experiment with this long CSP sample using shorter pump pulses of ~500 ps duration, which was realized subsequently using a different pump source at the site of the Bright partner confirmed, however, the extremely low OPG threshold. Having in mind the large refractive index of CSP (~3.2) OPO feedback should not be possible in this case for a crystal length exceeding 20 mm.

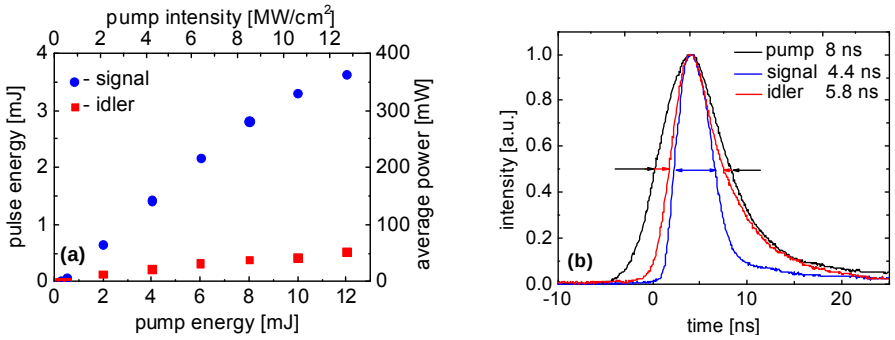

Figure 16: Signal (1288 nm) and idler (6.125 μm) output energy, and average power at 100 Hz versus incident pump energy at 1064 nm (a). Pump, signal and idler temporal shapes at maximum output energy (b): The numbers indicate the FWHM.

The temporal pulse profiles for the present set-up were measured using fast photo-detectors and are shown in Fig. 16b. The recorded idler profile is possibly affected by the 2.6 ns response time of the HgCdTe photoconductive detector. As expected the signal and idler have shorter pulse durations of 4.4 and 5.8 ns, respectively, than the pump.

The spatial properties of the OPO output beams were measured by a 10-cm MgF_2 focusing lens. Estimating the beam diameter with the knife-edge method gave M^2 values of 7.1 and 7.8 for the idler in the horizontal and vertical directions, respectively.

Taking into account the maximum signal pulse energy obtained with the present double-pass CSP-based OPG, a quantum conversion efficiency of 34.7% (or ~25% if the idler is considered which experiences some losses) is obtained. Before the onset of saturation, e.g. at a pump power of 6 mJ, these efficiencies amount to 41.4% and ~31%, respectively. All these values are much higher than the OPO quantum conversion efficiency achieved with a shorter crystal length of ~1 cm (this sample did not operate as OPG up to the highest pump level applied) that amounted to 12.8% using for the calculation the idler output because the signal was resonated (experiment described in subsection 3.1). Moreover, maximum pump pulse energy and peak intensity were about two times higher in this OPO and so the risk of damage. We repeated the OPO experiment with CSP sample 17B at 100 Hz, with a pump beam profile shaped to a quasi flat-top in the same manner as in the OPG case but, although the average power increased, the quantum conversion efficiency remained at ~13% and the M^2 factor (~11) was even worse than in the present, to a greater extent OPG, configuration.

Therefore, it can be concluded that the OPG concept is feasible in the temporal regime between 1 and 10 ns for achieving higher output energies and average powers. This is especially true for highly nonlinear crystals that still exhibit residual absorption losses (at the pump and signal wavelengths) such as the CSP crystal which is still in the development stage.

In fact, the presence of residual crystal surface reflections is not something that should be necessarily avoided as far as power/energy scaling is concerned. On the contrary, the issues with the resistivity of the AR-coatings for CSP are still not resolved and present data on their effect on the surface damage threshold of CSP is not conclusive. This means that uncoated crystals of CSP with plane-parallel faces could be used for resonant enhancement of the OPG regime, simultaneously avoiding the necessity of AR-coatings, or one of the surfaces can be Au-coated, as previously demonstrated for ZGP, for retro-reflection of the three waves [8]. In any case such designs are especially suited for CSP because it is also the only non-oxide material that enables non-critical phase-matching and temperature tuning for pump wavelengths in the 1 μm spectral range.

Only normal incidence was studied in the present configuration since the cavity was as short as possible in order to reduce the OPG threshold. As demonstrated before (see subsection 3.1) temperature tuning to 6.45 μm does not have a serious effect on the output energy level.

4. BGS based OPO

The orthorhombic wide band-gap biaxial crystal BGS was employed in a 1064-nm pumped OPO generating pulse energies as high as 0.5 mJ in the 6-μm range with average power ~50 mW at 100 Hz.

Within WP1, the transparency range, refractive index, Sellmeier dispersion equations and nonlinear coefficients of orthorhombic BGS were studied, a new chalcogenide nonlinear crystal for the mid-IR, applicable also for 6.45 μm generation. It is a new addition to the only few non-oxide nonlinear crystals that are transparent above ~5 μm in the mid-IR and simultaneously possess sufficiently wide band-gap to be pumped at relatively short wavelengths, e.g. Nd:YAG laser at 1064 nm, without TPA. While the effective nonlinearity of BGS for such down-conversion process (d_{eff}~5.1pm/V) is roughly two times lower in comparison to the commercially available chalcopyrite AGS, the advantage of BGS is its much higher (by an order of magnitude) surface damage threshold. This property, which is related to the large band-gap value of BGS (3.54 eV) renders BGS similar to the isostructural LGS which was also studied (both *mm*2 point group), however, BGS seems much more convenient to grow in large sizes with good optical quality. In the last period of the project OPO operation in the mid-IR was achieved with BGS pumped at 1064 nm. Although we obtained OPO operation under similar conditions also with LGS, operation only 50% above threshold could be reached because of the high threshold. The latter is a direct consequence of the limited crystal length of 8 mm available and the smaller aperture. Hence, we describe here only the results obtained with the BGS sample which had larger dimensions.

The large size sample available for the present experiment (Fig. 17a) had a yellow tinge. The 14.05-mm long element had an aperture of 9.8×9.5 mm^2. It was cut in the x-z plane at θ=12° for oo-e type-I phase-matching with the 9.8-mm edge parallel to the *y*-axis (vertical in the present case). The single layer sapphire AR-coating was specified by the supplier (ELAN Ltd.) with reflectivity of 2-3% for the pump (1.064 μm) and signal (~1.3 μm) wavelengths. These values were confirmed by transmission

measurements of the AR-coated sample (Fig. 17b) taking into account that the crystal absorption (measured prior to coating) did not exceed 0.01 cm^{-1} at all three wavelengths. The obtained residual surface reflectivity at the idler wavelength near 6 μm (~15%) is thus totally attributed to Fresnel reflection, see Fig. 17.

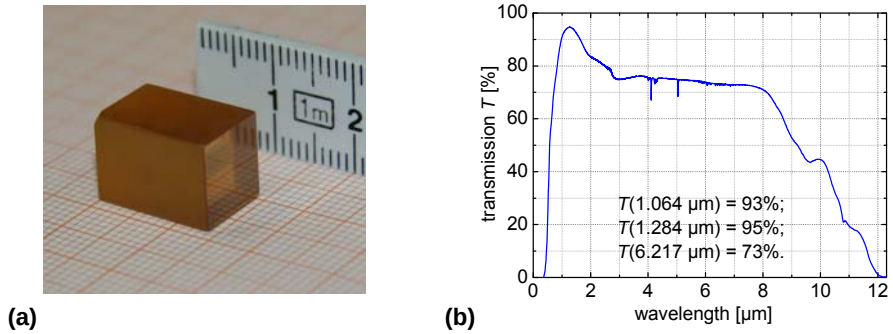

Figure 17: Photograph of the AR-coated BGS element (a) and transmission measured with unpolarized light (b).

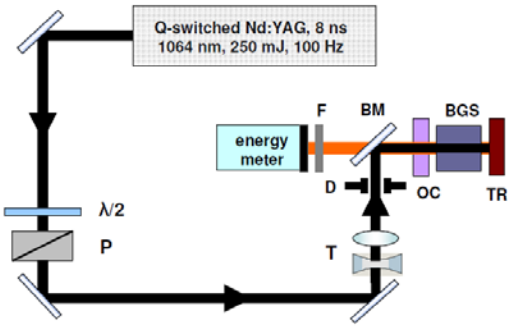

Figure 18: BGS OPO experimental set-up.

The OPO was pumped by the same 8-ns, 1064 nm upgraded pump source described before, delivering up to 250 mJ per pulse at 100 Hz, Fig. 18. A telescope (T) was applied to expand it to a diameter of ~5.5 and ~8.8 mm in the horizontal and vertical directions, respectively. The pump beam reached the BGS crystal after reflection at the ZnSe bending mirror (BM) and passing through the plane output coupler (OC) which transmitted 82%. The OC had a transmission of 18-22% at the signal wave and ~73-84% in the idler tuning range. An Ag-mirror was used as a total reflector (TR) for all three waves in a double pump pass singly resonant OPO configuration. The diaphragm (D) in Fig. 18 was used for alignment and the filters (F) were used for suppression of the residual pump and signal pulses.

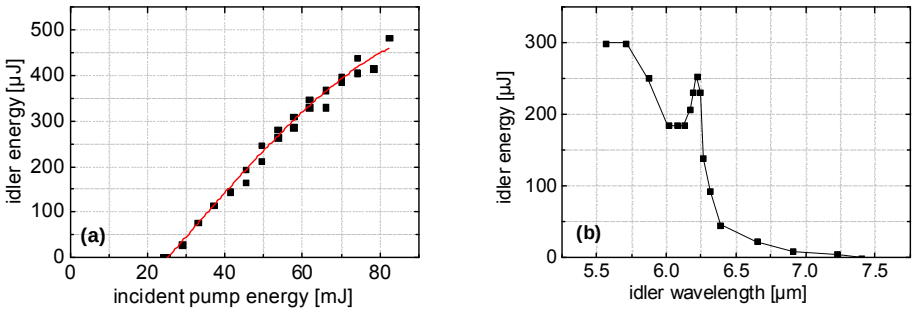

Figure 19: Input-output characteristics of the BGS OPO at normal incidence for a cavity length of 17 mm (a) and tuning characteristics for a cavity length of 20 mm recorded at an incident pump energy of 58 mJ (b).

Figure 19a shows the input-output characteristics obtained at normal incidence for a minimum cavity length of 17 mm. The threshold of 25 mJ corresponds to an axial fluence of 0.134 J/cm^2 or a peak

intensity of 16.7 MW/cm^2. The slope efficiency in the initial stage is ~1% with respect to the idler output but some saturation can be seen at higher powers. Nevertheless, an average idler power of ~50 mW was obtained at 100 Hz. The idler wavelength was 6.217 μm, in excellent agreement with calculations. The M^2 factor measured for the idler amounted to ~10. The OPO linewidth, measured at the signal wavelength using a 1-mm-thick Ag-coated CaF_2 Fabry-Perot etalon, was ~60 GHz (~2 cm^{-1}). In the present experiment the limit was set by damage of the Ag mirror which occurred at >50 MW/cm^2 peak pump intensity. Nevertheless, it was possible to reach three times above threshold pumping of the OPO.

Tuning was studied by tilting the crystal at slightly lengthened cavity (Fig. 19b). The idler wavelength range extended from 5.6 to 7.3 μm with a pronounced enhancement at normal incidence due to the idler reflection by the crystal surfaces. The minimum idler wavelength reached at θ=0° (uncritical interaction) was 5.6 μm.

The obtained results prove that chalcogenide nonlinear crystals with relatively low nonlinearity but wide band-gap and high damage resistivity are also very attractive for OPOs pumped at 1064 nm for frequency conversion to the mid-IR above ~5 μm. In fact, comparing with previous experience with crystals of AGS and LISe, with the present BGS crystal it was possible to reach the highest ratio of pump power above threshold (~3) without surface damage. Thus it was possible to reach with BGS the same level of idler pulse energy as with the highly nonlinear (more than 15 times higher nonlinearity) CSP (see subsection 3.1) for which the threshold in terms of pump energy was lower by about an order of magnitude. Since there were no thermal problems with BGS and no cumulative damage occurred, there was no problem to pump it also at a repetition rate of 100 Hz (most previous experiments with such 1064 nm pumped chalcogenide crystals were performed at 10 Hz) achieving the highest ever average powers (~50 mW) in the 6-μm spectral range with such an OPO.

5. Summary

Summarizing, the newly discovered CSP crystal seems predestined for the three-wave frequency conversion process under consideration, possessing a number of advantages and unique features such as non-critical phase-matching and temperature tuning capability to reach 6.45 μm. However, this type of phase-matching is not compatible with the RISTRA OPO cavity concept, successfully expolited by partners ISL and KTH for critical phase-matching pumping at longer wavelengths and the tunability is in general limited. On the other hand, the very high nonlinearity of CSP makes also the OPG concept feasible and allows one to achieve much better conversion efficiency even for pulse durations of the order of 10 ns available from commercial 1064 nm pump sources. While the further progress with CSP will depend on the reduction of residual losses and solution of the surface damage problem which is related to the AR-coatings, extremely wide band-gap nonlinear crystals as BGS show intrinsically low losses and much higher damage thereshold which enable also reaching relatively high output energies at 6.45 μm, albeit at a much higher threshold. The further progress with crystals like BGS or LGS will depend on the growth of larger sizes with sufficient optical quality.

6. References

[1] J.-J. Zondy, V. Vedenyapin, A. Yelisseyev, S. Lobanov, L. Isaenko, V. Petrov, "$LiInSe_2$ nanosecond optical parametric oscillator," Opt. Lett. **30**, 2460-2462 (2005).

[2] S. J. Brosnan, R. L. Byer, "Optical parametric oscillator threshold and linewidth studies," IEEE J. Quantum. Electron. **QE-15**, 415-431 (1979).

[3] V. Petrov, F. Noack, I. Tunchev, P. Schunemann, K. Zawilski, "The nonlinear coefficient d_{36} of $CdSiP_2$," Proc. SPIE **7197**, 7197-21/1-8 (2009).

[4] K. L. Vodopyanov, J. P. Maffetone, I. Zwieback, and W. Rudermann, "$AgGaS_2$ optical parametric oscillator continuously tunable from 3.9 to 11.3 μm," Appl. Phys. Lett. **75**, 1204-1206 (1999).

[5] A. V. Smith, D. J. Armstrong, "Nanosecond optical parametric oscillator with 90° image rotation: design and performance," J. Opt. Soc. Am. B **19**, 1801-1814 (2002).

[6] D. J. Armstrong, A. V. Smith, "All solid-state high-efficiency tunable UV source for airborne or satellite-based ozone DIAL systems," IEEE J. Sel. Top. Quantum Electron. **1**3, 721-731 (2007).

[7] A. Dergachev, D. Armstrong, A. Smith, T. Drake, M. Dubois, "3.4-μm ZGP RISTRA nanosecond optical parametric oscillator pumped by a 2.05-μm Ho:YLF MOPA system," Opt. Express **15**, 14404-14413 (2007).

[8] K. L. Vodopyanov, P. G. Schunemann, "Broadly tunable noncritically phase-matched $ZnGeP_2$ optical parametric oscillator with 2-μJ pump threshold," Opt. Lett. **28**, 441-443 (2003).

7. List of relevant publications in journals

1. V. Petrov, F. Noack, I. Tunchev, P. Schunemann, K. Zawilski, "The nonlinear coefficient d_{36} of $CdSiP_2$", *Proc. SPIE* **7197**(2009) 71970M/1-8.
2. G. Marchev, A. Tyazhev, V. Vedenyapin, D. Kolker, A. Yelisseyev, S. Lobanov, L. Isaenko, J.-J. Zondy, V. Petrov, "Nd:YAG pumped nanosecond optical parametric oscillator based on $LiInSe_2$ with tunability extending from 4.7 to 8.7 μm", *Opt. Express* **17**(2009) 13441-13446
3. V. Petrov, P. G. Schunemann, K. T. Zawilski, T. M. Pollak, "Noncritical singly resonant optical parametric oscillator operation near 6.2 μm based on a $CdSiP_2$ crystal pumped at 1064 nm", *Opt. Lett.* **34**(2009) 2399-2401
4. G. Marchev, A. Tyazhev, V. Vedenyapin, D. Kolker, A. Yelisseyev, S. Lobanov, L. Isaenko, J.-J. Zondy, V. Petrov, "Broadly tunable $LiInSe_2$ optical parametric oscillator pumped by a Nd:YAG laser", *Proc. SPIE* **7487**(2009) 74870F/1-9
5. A. Tyazhev, G. Marchev, V. Vedenyapin, D. Kolker, A. Yelisseyev, S. Lobanov, L. Isaenko, J.-J. Zondy, V. Petrov, "$LiInSe_2$ nanosecond optical parametric oscillator tunable from 4.7 to 8.7 μm", *Proc. SPIE* **7582**(2010) 75820E/1-11
6. V. Petrov, G. Marchev, P. G. Schunemann, A. Tyazhev, K. T. Zawilski, T. M. Pollak, "Subnanosecond, 1 kHz, temperature-tuned, noncritical mid-infrared optical parametric oscillator based on $CdSiP_2$ crystal pumped at 1064 nm", *Opt. Lett.* **35**(2010) 1230-1232.
7. V. Petrov, J.-J. Zondy, O. Bidault, L. Isaenko, V. Vedenyapin, A. Yelisseyev, W. Chen, A. Tyazhev, S. Lobanov, G. Marchev, D. Kolker, "Optical, thermal, electrical, damage, and phase-matching properties of lithium selenoindate," *J. Opt. Soc. Am. B* **27**(2010) 1902-1927.
8. V. Badikov, D. Badikov, G. Shevyrdyaeva, A. Tyazhev, G. Marchev, V. Panyutin, V. Petrov, A. Kwasniewski, "Phase-matching properties of $BaGa_4S_7$ and $BaGa_4Se_7$: Wide-bandgap nonlinear crystals for the mid-infrared," *Phys. Stat. Sol. RRL* **5**(2011) 31-33.
9. V. Vedenyapin, L. Isaenko, A. Yelisseyev, S. Lobanov, A. Tyazhev, G. Marchev, V. Petrov, "New mixed $LiGa_{0.5}In_{0.5}Se_2$ nonlinear crystal for the mid-IR," *Proc. SPIE* **7917**(2011) 79171L/1-8.
10. A. Yelisseyev, M. Starikova, L. Isaenko, S. Lobanov, V. Petrov, "Effect of post-growth annealing on the optical properties of $LiGaS_2$ nonlinear crystals," *Proc. SPIE* **7917**(2011) 79171S/1-8.
11. V. Badikov, D. Badikov, G. Shevyrdyaeva, A. Tyazhev, G. Marchev, V. Panyutin, F. Noack, V. Petrov, A. Kwasniewski, "$BaGa_4S_7$: wide-bandgap phase-matchable nonlinear crystal for the mid-infrared," *Opt. Mater. Express* **1**(2011) 316-320.
12. V. Kemlin, B. Boulanger, V. Petrov, P. Segonds, B. Ménaert, P. G. Schunneman, K. T. Zawilski, "Nonlinear, dispersive, and phase-matching properties of the chalcopyrite $CdSiP_2$," *Opt. Mater. Express* **1**(2011) 1292-1300.
13. V. Petrov, "Parametric down-conversion devices: The coverage of the mid-infrared spectral range by solid-state laser sources," *Opt. Mater.* **34**(2012) 536-554.
14. G. Marchev, A. Tyazhev, G. Stöppler, M. Eichhorn, P. Schunemann, V. Petrov, "Comparison of linear and RISTRA cavities for a 1064 nm pumped $CdSiP_2$ OPO," *Proc. SPIE* **8240**(2012), in press.
15. G. Marchev, A. Tyazhev, V. Petrov, P. G. Schunemann, K. T. Zawilski, G. Stöppler, M. Eichhorn, "Optical parametric generation in $CdSiP_2$ at 6.125 μm pumped by 8-ns long pulses at 1064 nm," *Opt. Lett.* **37**(2012), in press.